ELECTRICAL PROPERTIES OF NANOSCALE HETEROJUNCTIONS FORMED BETWEEN GaN AND ZnO NANORODS

TIAGULSKYI Stanislav[1], YATSKIV Roman[1], GRYM Jan[1], SCHENK Antonín[1], ROESEL David[1], VANIŠ Jan[1], HAMPLOVA Marie[1]

[1]*Institute of Photonics and Electronics of the Czech Academy of Sciences, Prague, Czech Republic, EU*

Abstract

Vertical periodic arrays of ZnO nanorods are prepared by hydrothermal growth on GaN templates patterned by focused ion beam. Electro-physical properties of a single vertically-oriented ZnO nanorod are investigated by measuring the current-voltage characteristics using a nanoprobe in a scanning electron microscope. This technique enables to observe the surface morphology of ZnO nanorods simultaneously with their electrical characterization in vacuum. The vacuum chamber rejects the impact of gas adsorption and light irradiation, which both affect the properties of ZnO nanorods. Moreover, mechanical damage and strain induced during the nanorod transfer are eliminated. Nonlinear current-voltage characteristics under the forward bias are explained by the tunneling-recombination process and by the space charge limited current. The high reverse bias current in the p-n heterojunction is attributed to direct tunneling via a narrow tunnel barrier.

Keywords: Hydrothermal growth, nanoscale heterojunctions, in-situ current-voltage measurements, nanomanipulator, scanning electron microscope, ZnO/GaN heterojunction, ZnO nanorod

1. INTRODUCTION

Nanoscale heterostructures are promising functional components for a new generation of electronic and photonic devices. The high demand for the light-emitting devices, photodetectors, solar cells, and gas sensors increases interest in the development of the nanoscale heterostructures [1]. ZnO nanorods (NR) are particularly appropriate candidates for the fabrication of nanoscale p-n heterojunctions. ZnO is an abundant wide-bandgap (3.37 eV at room temperature) semiconductor with the large exciton binding energy (60 meV). It crystallizes in the wurtzite structure with a close match to GaN lattice [2]. Moreover, it easily forms several types of nanostructures that are suitable for the manufacturing of vertically stacked devices [3].

In this work, electro-physical properties of a single vertically-oriented hydrothermally grown ZnO NR on GaN templates are investigated by measuring the current-voltage (I-V) characteristics. The contact to a single NR is obtained by a nanoprobe in the chamber of a scanning electron microscope (SEM), which allows for a simultaneous measurement of the I-V characteristics and observation of the surface morphology. Moreover, using this technique we eliminated the influence of (a) a surrounding dielectric and/or neighboring NRs (as in the case of the NR array) [4], (b) the impact of the gas adsorption [5] and light illumination [6], (c) the strain induced during the ZnO NR transfer to other substrates [7].

2. EXPERIMENTAL METHODS

The ZnO NRs were grown hydrothermally in a 5mM aqueous solution of zinc nitrate hexahydrate and hexamethylenetetramine at 95 °C for 2 hours on epitaxial layers of p-GaN:Mg on sapphire (HVPE; Kyma, Inc.) [8]. The thickness of the GaN epi-layer was 2 μm, the acceptor concentration $N_A = 5 \cdot 10^{17}$ cm^{-3}. To create a back ohmic contact (**Figure 1a**) a 50 nm film of Ni covered with a 40 nm film of Au was thermally evaporated on the p-GaN surface through a simple mask with circular holes and was subsequently annealed at 500 °C. Prior the growth of ZnO NRs, the GaN film was thoroughly cleaned using a standard procedure of ultrasonic bathing in acetone with subsequent etching in concentrated ammonium hydroxide solution (28%, 50 °C,

20 min). Further, a 200 nm poly(methyl methacrylate) (PMMA) film was deposited by spin-coating. Ga^+ focused ion beam (FIB) was employed to fabricate the array of circular holes in the PMMA layer. The acceleration voltage was 30 keV and the probe current was 57 pA. The patterned PMMA layer served directly as a lithographic mask. A standard lift-off procedure was performed after the growth process. The control of the size and morphology of the ZnO NR was carried out using the Tescan Lyra 3 GM FIB/SEM system. The I-V characteristics of the nanoscale heterojunction formed by a single n-type ZnO NR on p-type GaN substrate) were measured in the chamber of SEM using a SmarAct nanoprobe with a tungsten tip (**Figure 1b**) and Keithley 236/237 measure unit driven by the lab-made script (Python 3.6).

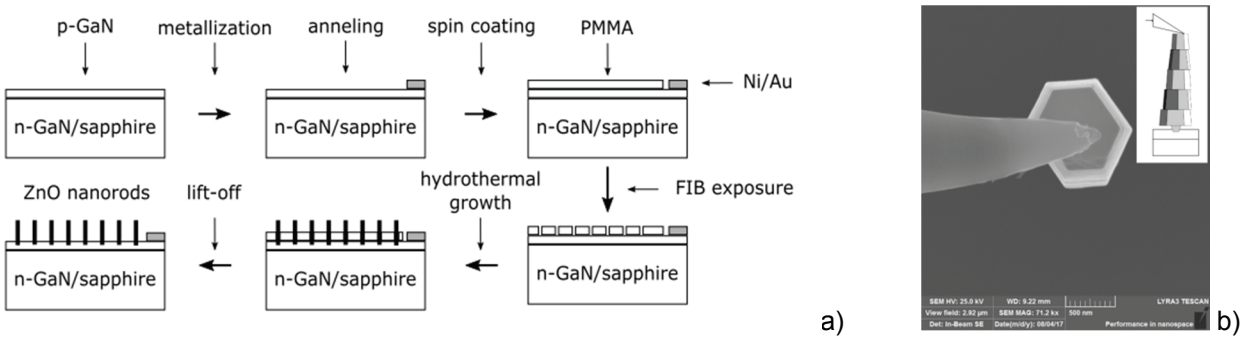

Figure 1 (a) Flowchart of the fabrication process of the arrays of ZnO NRs and (b) SEM images of the individual hexagonal monocrystalline ZnO NR contacted by the nanoprobe. The inset shows schematically the twist and shear deformation of a ZnO NR under stress imposed by the nanoprobe.

3. RESULTS AND DISCUSSION

3.1. Current-voltage measurements of n-ZnO/p-GaN heterojunctions

The wiring diagram for the electrical characterization of individual ZnO NRs is shown in **Figure 2a**. According to simple Anderson model, the n-ZnO/p-GaN heterojunction has type II band alignment with the band discontinuities ΔE_c = 0.15 eV, ΔE_v = 0.13 eV [9].

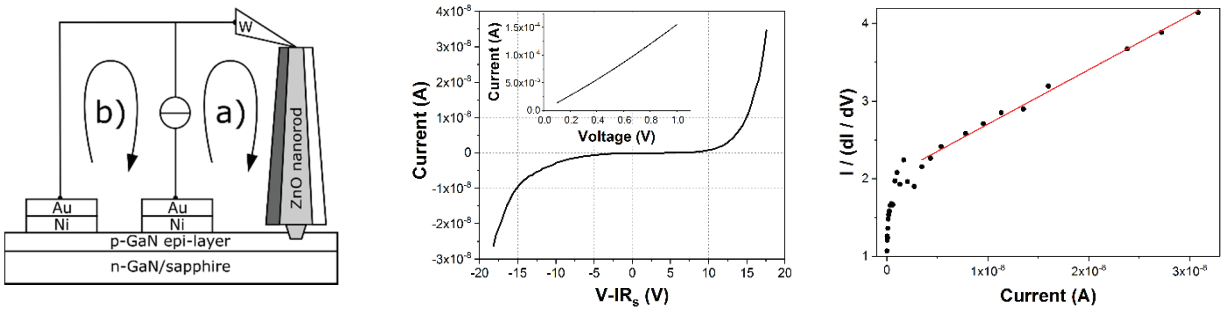

Figure 2 The scheme for the I-V measurement of single ZnO NR (a), the I-V characteristic of the nanoscale n-ZnO NR / p-GaN heterojunction (b), inset - the I-V curve of Ni / p-GaN / Ni, the plot of $I\,{}^{dI}/_{dV}$ vs. I (c)

Figure 2b shows an I-V characteristic of the nanoscale heterojunction between a single n-ZnO NR and p-GaN epitaxial substrate measured at room temperature in the vacuum chamber of SEM. A negative voltage applied to the nanoprobe is considered as a forward biased p-n junction and vice versa. The I-V curve has a non-linear moderately asymmetrical shape that is typical for the diode with a low rectification ratio (1:1 at ± 4 V and 34:1 at ± 15 V) and a large leakage current. The turn-on voltage V_{on} was ≈ 4 V, which corresponds to previously reported values [9]. The leakage current under reverse bias of -4 V was I_{leak} ≈ 4.7 pA and the corresponding current density J_{leak} ≈ $1.2 \cdot 10^{-3}$ A/cm^2.

A simple Schottky model [10] predicts an ohmic contact between the tungsten tip and the ZnO NR. The linear I-V curve was measured between two Ni/Au contacts. Hence, the behavior of I-V characteristics is determined by the transport through the heterojunction and/or by the properties of the ZnO NR rather than by the metal-semiconductor interfaces. A standard approach to characterize electric transport in semiconductor devices is to re-plot the measured I-V curve in the some characteristic coordinates. The thermionic emission [11], Fowler-Northeim tunneling [12], electron-hole recombination process [13], space charge limited current (SCLC) [14], hopping conduction [15] were observed in single semiconductor nanowires. However, the series resistance should be excluded from the experimental I-V characteristic prior analyzing the electric transport mechanism [9]. The I-V characteristics of a semiconductor diode are generally expressed as:

$$I \sim \exp\left(\frac{q(V-IR_S)}{nkT}\right) - 1, \; n = \frac{q}{kT}\frac{dV}{d(lnI)}, \tag{1}$$

where V and I are the applied voltage and measured current, q is the electron charge, R_s is the series resistance, k is Boltzmann constant, n is the ideality factor, T is the temperature [16]. The series resistance has been extracted from the linear fit of experimental I-V curve using the following equation:

$$I\,{}^{dI}/_{dV} = R_s I + {}^{kT}/_{q} \text{ for } V > {}^{kT}/_{q}, \tag{2}$$

where q is the elementary charge. The plot of $I\,{}^{dI}/_{dV}$ versus current is a straight line as shown in **Figure 2c**. The slope of the line gives the value of $R_s \approx 7 \cdot 10^7$ Ohm.

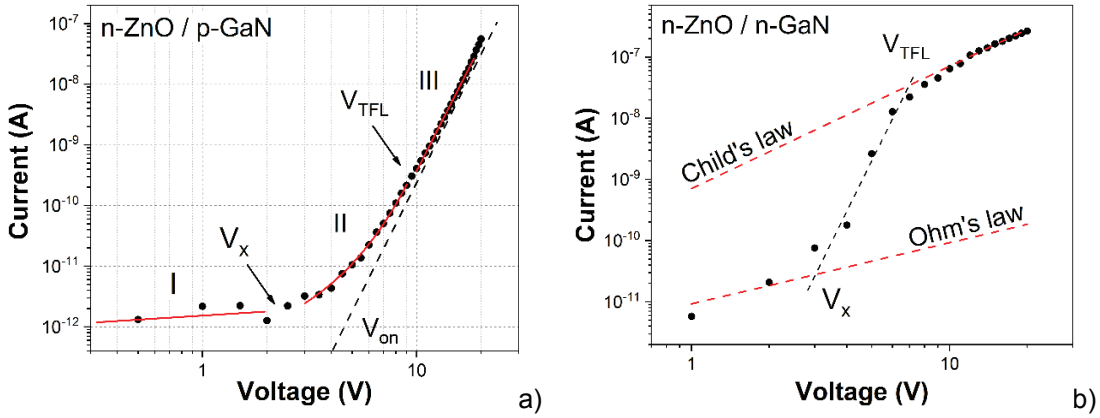

Figure 3 The forward log-log I-V characteristics of the p-n (a) and n-n (b) ZnO/GaN heterojunctions

Figure 3a shows *I-V* characteristic of the nanoscale n-ZnO/p-GaN heterojunction in the logarithmic scale. The forward I-V characteristic can be divided into three regions: linear (I), exponential (II), and power-law (III). By applying equation (1) to the exponential part (II) of the curve, the ideality factor n is found to be 49. Larger than unity ideality factors are commonly observed in the devices based on ZnO NRs and are generally associated with defects and inhomogeneity or non-linearity of the nanoscale metal contacts [12].

Moreover, the contact by the nanoprobe tip has additional specific impact on the electrical transport in individual vertical semiconductor NRs. Overpressure by the NM introduces deformations to the NRs. Using X-ray nano-diffraction, Bussone et al. proved appearance of shear and twist deformations (inset in **Figure 1b**) after contacting a NR using a tungsten tip [17]. The deformation was considered as a source of additional intrinsic interfaces within the semiconductor NR that increase total ideality factor of the device. Moreover, there are theoretical models that explain anomalously high ideality factors by serial connection of several segments of inhomogeneous nanocontacts with a different resistivity [18].

The tunneling-recombination process is considered as the main transport mechanism for wide bandgap semiconductor heterojunctions [19]. Applying tunneling-recombination formalism to analyze the forward I-V characteristics of our structures, we fitted a corresponding region of the I-V curve with the expression:

$$I \approx \exp(\alpha V)\,,\ \alpha = ({}^{8\pi}/_{3h})(m_h^*\varepsilon)^{1/2}N_D\left[N_A^{1/2}(N_A+N_D)\right] \quad (3)$$

Where α is the injection efficiency coefficient, h is the Plank constant, m_h^* is the effective hole mass, ε is the dielectric constant, N_D is the donor concentration in n-ZnO, N_A is the acceptors concentration in the p-GaN. The value of α = 0.77 is moderately lower than reported before [20]. Using equation (3) the concentration of donor impurities N_D was found to be $3\cdot10^{16}$ cm^{-3}. This value is in a good agreement with N_D = $1.24\cdot10^{16}$ cm^{-3} obtained before for the hydrothermally grown ZnO NRs [21]. With increasing applied voltage the crossover between exponential and power-law regions of the I-V curve is observed at V_{TFL} = 9.5 V. The power-law I-V characteristic with the power factor a >> 2 is related to charge transport limited by the trap filling process (TFL) [22]. The crossover voltage V_{TFL} is defined as a voltage required to fill the traps, or in other words, as a voltage at which quasi-Fermi level passes through the trap level (or average energy associated with the traps density). By further increase of the applied voltage, the I-V characteristic should follow the regime of SCLC when the factor of power law is equal 2. We did not observe the TFL/SCLC crossover in our NR p-n heterojunctions. It could be related to insufficient efficiency of the injection and low free carrier concentration due to the non-ideal nanocontact, high trap concentration, or surface carrier depletion in the structures of small dimensions.

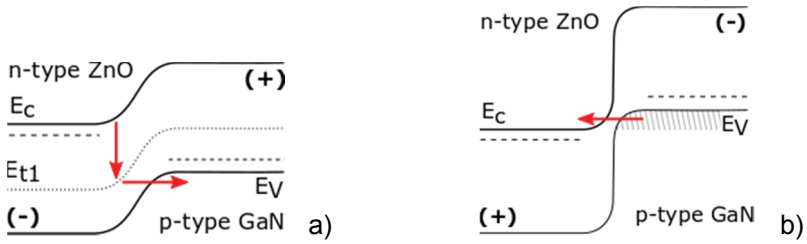

Figure 4 Schematic diagrams of the current transport in n-ZnO/p-GaN heterojunction under (a) forward and (b) reverse bias

The reverse I-V characteristics could be quantitatively explained by direct tunneling mechanism [23]. When the applied reverse bias overcomes the breakdown voltage V_{br} ≈ 6V (**Figure 2c**), the overall band structure of the p-GaN film is elevated, leading to a near broken-gap band alignment (type III) with the narrow tunnel barrier at the p-n junction (**Figure 4b**). Then, electrons from the filled states in the valence band of p-GaN travel to the aligned empty conduction band states on n-ZnO through the barrier. However, our reverse I-V curve does not fit well the expression of the Zener tunneling law. Therefore, additional factors that affect transport in nanoscale heterojunctions (nanocontact inhomogeneity, tunneling through the defects, parasitic leakages etc.) should be carefully considered in the future.

3.2. Current-voltage measurements of isotype n-ZnO/n-GaN heterojunctions

Additionally, the isotype n-ZnO NR/n-GaN heterojunctions were investigated. These structures were grown under the same conditions as the p-n heterojunction described before. Due to the absence of potential drops on contacts and interfaces, the structures demonstrate electric transport limited by the semiconductor NR space charge region [14] rather than by metal/semiconductor or heterojunction interfaces. The forward I-V characteristics of the isotype n-ZnO NR/n-GaN heterojunction in log-log coordinates shows several distinct regions (**Figure 3b**). At a low bias when the injected electron concentration is small compared to the equilibrium electron concentration n_0, the current follows the Ohm's law:

$$I \approx qn_0\mu\frac{V}{L}, \quad (4)$$

where μ is the electron mobility, L is the NR length. The next region (II in **Figure 3b**) with the power law coefficient a > 2 corresponds to the SCLC regime with the unfiled traps (trap-SCLC). The following high-slope region (III in **Figure 3b**) with the power law coefficient a=7 corresponds to crossover process limited by TFL.

Further, at the highest bias (IV in **Figure 3b**), the trap-free SCLC regime with a=2 is observed. The SCL current density in the nanowires follows the Child's law [14]:

$$J = {}^{I}/_{\pi r^2} \approx (\frac{r}{L})^{-2}\varepsilon_0\varepsilon\mu\frac{V^2}{L^3} \text{ for } L/r \geq 5, \quad (5)$$

where *r* and *L* are the radius and the length of the nanowire, ε_0 is the permittivity of free space, ε is the relative dielectric constant of a nanowire. The reason for the high SCLC current density in a nanowire is the poor electrostatic screening that the injected carriers experience in a high aspect ratio conductor (which is surrounded by air or vacuum) [4]. Fitting the region IV of the experimental I V curve with equation (5) the electron mobility μ was found to be 0.15 $cm^2/V{\cdot}s$. Using obtained value of μ for the fitting of the region I with the equation (4) the effective free carrier concentration n_0 was found to be $5{\cdot}10^{13}$ cm^{-3}. Otherwise, effective concentration of free carriers is given as:

$$n_0 = N_C \exp\left[{}^{(E_F - E_C)}/_{kT}\right], \quad (6)$$

where $N_C \approx 4.8{\cdot}10^{18}$ cm^{-3} is the effective density of states for ZnO at room temperature [24]. Hence, the position of the effective Fermi level (E_f - E_c) was estimated as 0.65 eV. However, this position of effective Fermi level could not be explained by a single trap level. Thus, we suggest wide distribution of trap levels over the bandgap. The TFL / SCLC crossover voltage V_{TFL} is given as:

$$V_{TFL} = {}^{N_t q L}/_{2\varepsilon\varepsilon_0}, \quad (7)$$

where N_t is the trap concentration, located at the estimated effective Fermi level [22]. Using $V_{TFL} \approx 7$ V the effective concentration of traps N_t was found to be $4.9{\cdot}10^{14}$ cm^{-3}.

4. CONCLUSIONS

The nanoscale ZnO NR/GaN heterojunctions were synthesized by hydrothermal growth. The I-V characteristics of individual ZnO NRs were measured using nanoprobe with a tungsten tip in the chamber of a scanning electron microscope. Both metal-semiconductor contacts showed ohmic behavior. However, the non-ideality/inhomogeneity of the top nanocontact should be taken into account. In general, the nonlinear I-V characteristic on the forward bias is explained by the tunneling-recombination process or by the space charge limited current depending on the type of the junction and on the applied bias. The high reverse bias current in the p-n heterojunction was attributed to direct tunneling transport via a narrow tunnel barrier. The electrical parameters of single ZnO NRs illustrate commonly observed behavior, where the low electron mobility is explained by a high concentration of defects related to the ZnO/GaN lattice mismatch (≈ 1.9%) and the low temperature ZnO NR growth. The low free carrier concentration is associated with the low doping level or carrier depletion due to the trapping on the surface states in low-dimensions structures.

ACKNOWLEDGMENTS

This work was supported by the Czech Science Foundation projects: 17-00546S and 15-17044S.

REFERENCES

[1] BARTH, S., HERNANDEZ-RAMIREZ, F., HOLMES, J. D. and ROMANO-RODRIGUEZ, A. Synthesis and applications of one-dimensional semiconductors. *Progress in Materials Science,* 2010, vol. 55, no. 6, pp. 563-627.

[2] JANOTTI, A. and VAN DE WALLE, C. G. Fundamentals of zinc oxide as a semiconductor. *Reports on Progress in Physics,* 2009, vol. 72, no. 12, p. 29.

[3] OZGUR, U., ALIVOV, Y. I., LIU, C., TEKE, A., RESHCHIKOV, M. A., DOGAN, S., AVRUTIN, V., CHO, S. J. and MORKOC, H. A comprehensive review of zno materials and devices. *Journal of Applied Physics,* 2005, vol. 98, no. 4, p. 103.

[4] MALLAMPATI, B., SINGH, A., SHIK, A., RUDA, H. E. and PHILIPOSE, U. Electro-physical characterization of individual and arrays of zno nanowires. *Journal of Applied Physics,* 2015, vol. 118, no. 3, p. 6.

[5] YATSKIV, R., GRYM, J., GLADKOV, P., CERNOHORSKY, O., VANIS, J., MAIXNER, J. and DICKERSON, J. H. Room temperature hydrogen sensing with the graphite/zno nanorod junctions decorated with pt nanoparticles. *Solid-State Electronics,* 2016, vol. 116, pp. 124-129.

[6] YATSKIV, R., GRYM, J. and VERDE, M. Graphite/zno nanorods junction for ultraviolet photodetectors. *Solid-State Electronics,* 2015, vol. 105, pp. 70-73.

[7] SAKURAI, M., WANG, Y. G., UEMURA, T. and AONO, M. Electrical properties of individual zno nanowires. *Nanotechnology,* 2009, vol. 20, no. 15, p. 6.

[8] YATSKIV, R. and GRYM, J. Well-aligned zno nanorods grown directly on gan substrates for optoelectronic applications, In *2016 IEEE 11th Annual International Conference on Nano/Micro Engineered and Molecular Systems*, *NEMS,* 2016, p. 176.

[9] KONG, B. H., HAN, W. S., KIM, Y. Y., CHO, H. K. and KIM, J. H. Heterojunction light emitting diodes fabricated with different n-layer oxide structures on p-gan layers by magnetron sputtering. *Applied Surface Science,* 2010, vol. 256, no. 16, pp. 4972-4976.

[10] REDDY, N. K., AHSANULHAQ, Q., KIM, J. H., DEVIKA, M. and HAHN, Y. B. Selection of non-alloyed ohmic contacts for zno nanostructure based devices. *Nanotechnology,* 2007, vol. 18, no. 44, p. 6.

[11] HEO, Y. W., TIEN, L. C., NORTON, D. P., PEARTON, S. J., KANG, B. S., REN, F. and LAROCHE, J. R. Pt/zno nanowire schottky diodes. *Applied Physics Letters,* 2004, vol. 85, no. 15, pp. 3107-3109.

[12] KIM, K., KANG, H., KIM, H., LEE, J. S., KIM, S., KANG, W. and KIM, G. T. Contact barriers in a single zno nanowire device. *Applied Physics a-Materials Science & Processing,* 2009, vol. 94, no. 2, pp. 253-256.

[13] LEONARD, F., TALIN, A. A., SWARTZENTRUBER, B. S. and PICRAUX, S. T. Diameter-dependent electronic transport properties of au-catalyst/ge-nanowire schottky diodes. *Physical Review Letters,* 2009, vol. 102, no. 10, p. 4.

[14] TALIN, A. A., LEONARD, F., SWARTZENTRUBER, B. S., WANG, X. and HERSEE, S. D. Unusually strong space-charge-limited current in thin wires. *Physical Review Letters,* 2008, vol. 101, no. 7, p. 4.

[15] CHIU, S. P., LIN, Y. H. and LIN, J. J. Electrical conduction mechanisms in natively doped zno nanowires. *Nanotechnology,* 2009, vol. 20, no. 1, p. 8.

[16] SCHRODER, D. K. *Semiconductor material and device characterization*, *3* ed. New York: John Wiley & Sons, 2006, pp. 800.

[17] BUSSONE, G., SCHAFER-EBERWEIN, H., DIMAKIS, E., BIERMANNS, A., CARBONE, D., TAHRAOUI, A., GEELHAAR, L., BOLIVAR, P. H., SCHULLI, T. U. and PIETSCH, U. Correlation of electrical and structural properties of single as-grown gaas nanowires on si (111) substrates. *Nano Letters,* 2015, vol. 15, no. 2, pp. 981-989.

[18] FERNANDES, C., SHIK, A., BYRNE, K., LYNALL, D., BLUMIN, M., SAVELIEV, I. and RUDA, H. E. Axial p-n-junctions in nanowires. *Nanotechnology,* 2015, vol. 26, no. 8, p. 8.

[19] RIBEN, A. R. and FEUCHT, D. L. Electrical transport in nge-pgaas heterojunctions. *International Journal of Electronics,* 1966, vol. 20, no. 6, pp. 583-&.

[20] YE, J. D., GU, S. L., ZHU, S. M., LIU, W., LIU, S. M., ZHANG, R., SHI, Y. and ZHENG, Y. D. Electroluminescent and transport mechanisms of n-zno/p-si heterojunctions. *Applied Physics Letters,* 2006, vol. 88, no. 18, p. 3.

[21] YATSKIV, R., BRUS, V. V., VERDE, M., GRYM, J. and GLADKOV, P. Electrical and optical properties of graphite/zno nanorods heterojunctions. *Carbon,* 2014, vol. 77, pp. 1011-1019.

[22] LAMPERT, M. A. Simplified theory of space-charge-limited currents in an insulator with traps. *Physical Review,* 1956, vol. 103, no. 6, pp. 1648-1656.

[23] JEONG, J., CHOI, J. E., KIM, Y. J., HWANG, S., KIM, S. K., KIM, J. K., JEONG, H. Y. and HONG, Y. J. Reverse-bias-driven dichromatic electroluminescence of n-zno wire arrays/p-gan film heterojunction light-emitting diodes. *Applied Physics Letters,* 2016, vol. 109, no. 10, pp. 22-26.

[24] SZE, S. M. *Physics of semiconductor devices*, *3rd* ed. Hoboken, NJ: John Wiley and Sons, 2007, pp. 815.